International Journal of Applied Science and Engineering

Photonic crystal fibre sensor for alcohol detection with extremely low birefringence

Ang Chuan Shi[1], Abdul Mu'iz Maidi[1], Norazanita Shamsuddin[1], Md Abul Kalam[2], Feroza Begum[1*]

[1] *Faculty of Integrated Technologies, Universiti Brunei Darussalam, Jalan Tungku Link, Gadong, Bandar Seri Begawan BE1410, Brunei Darussalam*

[2] *Faculty of Engineering and Information Technology, University of Technology Sydney, 15 Broadway Ultimo, NSW 2007, Australia*

ABSTRACT

A photonic crystal fibre (PCF) based alcohol sensor with extremely low birefringence has been proposed for different alcohol analytes of propanol, butanol and pentanol, operating within 0.8 to 2.0 µm wavelength. A structural design of three layers of circular cladding air holes with three elliptical core holes has been designed and simulated to distinguish the capabilities of the PCF as a sensor, which accomplished high relative sensitivity, low confinement loss and extremely low birefringence. At the examined optimum wavelength of 0.8 µm, the assessed relative sensitivities are 93.3%, 88.7% and 82.2% for propanol, butanol and pentanol, respectively, and confinement losses of 9.80 × $1/10^{13}$ dB/m for propanol, 4.91 × $1/10^{13}$ dB/m for butanol and 1.03 × $1/10^{13}$ dB/m for pentanol. The birefringence of the proposed PCF is about 0.0001 for all the selected test analytes. Moreover, considering the simple cross-sectional design, it shall be easily fabricated for practical alcohol detection.

Keywords: Photonic crystal fibre, Alcohol sensor, Relative sensitivity, Confinement loss.

OPEN ACCESS

Received: October 19, 2022
Revised: January 6, 2023
Accepted: January 17, 2023

Corresponding Author:
Feroza Begum
feroza.begum@ubd.edu.bn

Copyright: The Author(s). This is an open access article distributed under the terms of the Creative Commons Attribution License (CC BY 4.0), which permits unrestricted distribution provided the original author and source are cited.

Publisher:
Chaoyang University of Technology
ISSN: 1727-2394 (Print)
ISSN: 1727-7841 (Online)

1. INTRODUCTION

Optical fibres are widely known for their applications in communications systems, and they can be categorised into several types, such as conventional optical fibres (COFs) and photonic crystal fibres (PCFs). PCFs are a prominent research topic due to their flexibility in different fields, mainly sensing applications (Hemalatha and Revathi, 2020; Maidi et al., 2022). Since the first discovery of PCF in 1996 (Knight et al., 1996), it has been used as an alcohol sensing channel due to its unique attribute in photonics and optoelectronics (Habib et al., 2017; Islam et al., 2018). Principally, the performance of a PCF is dependent on the complexity of the cladding and core structures. As a rule, more implementation of cladding air holes in the fibre structure shall produce better performance. A study (Nivedha and Senthilnathan, 2020) presented an alcohol sensor that mimics a steering wheel, implementing a porous core and cladding hole structure. The core design consists of multiple layers of nine rectangular holes arranged horizontally, enclosed by circular lattice cladding air holes. Additionally, a PCF sensor for ethanol detection has been introduced (Sultana et al., 2018), whereby the core formed in three elliptical hole columns in a vertical position. A standard and straightforward hexagonal structured PCF was proposed with a large core design of six oval holes for both inner and outer core regions, whereas the cladding region has three-layered circular air holes (Podder et al., 2020). An octagonal photonic crystal fibre (O-PCF) has also been demonstrated, featuring octagonal lattice cladding air holes of five layers with two layers of hexagonal core holes (Abdullah-Al-Shafi and Sen, 2020). Similarly, different researchers (Sen et al., 2021) introduced a similar porous core design but included a decagonal shaped photonic crystal fibre (D-PCF). Moreover, another research

(Iqbal et al., 2020) applied rectangular cladding air holes surrounding a single rectangular-shaped core for a PCF sensor.

Several studies involving alcohol content: propanol, butanol and pentanol have been researched in different PCF configurations. A group of researchers (Habib et al., 2021) brought forward an alcohol detection PCF sensor with the design of 5 cladding air holes rings and large circular core hole. With a such simple core design but numerous cladding holes, the PCF structure managed to attain relative sensitivities 80.74% for propanol and 84.34% for butanol, and confinement losses of about $1/10^{10}$ dB/m for propanol and butanol at 1.1 µm operating wavelength. With an integration of 5 layers cladding air holes, it comes at the disadvantage in the fabrication process. Ahmad et al. (Ahmed et al., 2017) have proposed two core designs: oval and circular holes. Firstly, the PCF sensor with circular core holes has assessed relative sensitivities of 65.95%, 66.35% and 66.73% for propanol, butanol and pentanol, respectively, at 1.55 µm operating wavelength. Conversely, the elliptical-cored PCF design deduced relative sensitivities of 58.17% for propanol, 58.74% for butanol and 59.29% for pentanol at the same wavelength of 1.55 µm. Although with elaborative designs of 5 layers cladding holes and 19 core holes, the relative sensitivities obtained are considerably low for sensing applications. Another group of researchers (Ahmed et al., 2019) has introduced a PCF alcohol sensor with a circular core and cladding structure. The air holes are arranged in an 'X' pattern, and gold coating imposed surrounding the cladding by a 1 µm analyte. The relative sensitivities for the PCF design of propanol, butanol and pentanol were below 50%, which are 41.29%, 41.30% and 41.32%, respectively, at an optimum wavelength of 1.5 µm. The drawback of this simple PCF design of fewer cladding air holes is minimal results for alcohol detection, as seen from the data of relative sensitivities. Furthermore, a PCF sensor of five circular rings of cladding air holes and two circular core rings have been proposed by Paul et al. (Paul et al., 2017). The test analytes for this porous-cored study are propanol, butanol and pentanol, which obtained relative sensitivities of 65.44%, 66.02% and 66.39%, respectively, at 0.8 µm operating wavelength. Due to the characteristics of porous core designs, challenges arise in the fabrication process that increases the probability in inaccuracy of the core holes dimensions.

From the literature (Ahmed et al., 2017, 2019; Paul et al., 2017), the structural design of the shape, orientation and arrangement of the core and cladding designs influences the results of relative sensitivities and confinement losses. Thus, a non-complex PCF design of low number cladding air holes and simple structural core design has been selected for alcohol sensing in this research. Three test analytes of propanol, butanol, and pentanol shall be infiltrated through the core holes for alcohol detection and assessing effective refractive index, birefringence, power fraction, relative sensitivity, confinement loss, effective area and nonlinear coefficient in the operating wavelength 0.8 to 2.0 µm.

2. DESIGN

Fig. 1 illustrates the structural design of the proposed PCF for alcohol detection of propanol, butanol and pentanol, whereby it is comprised of three layers: three elliptical core holes, cladding air holes of two layers and the Perfectly Matched Layer (PML). Light propagates through the elliptical core holes whilst the cladding air holes exist to restrict the light from escaping the core region of the fibre. Meanwhile, the outer PML is corrected to 10% of the fibre structure to allow absorption of leaked signal and prevent light from reflecting into the cladding. With intricate core and cladding designs implemented, the difficulty in the fabrication process will increase significantly as well. Therefore, the proposed model is kept at a simple design without compromising the capabilities of analyte sensing.

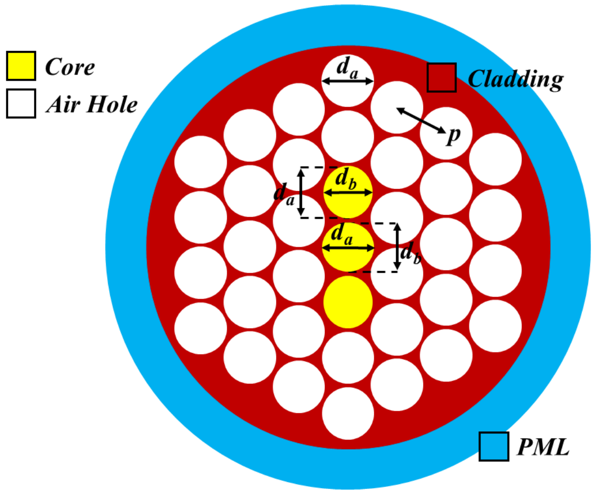

Fig. 1. Proposed design of PCF sensor

The core design of the proposed PCF includes three elliptical hollow holes with long axis diameter denoted as d_a and short axis diameter represented as d_b. The cladding air holes surrounding the core structure is comprised of two layers air-holes arranged in a hexagonal lattice. A total of thirty-four air holes exists in the cladding region with a diameter d_a, similar to the core hole diameter in the x-plane. The diameter d_a is specified to 4.0 µm, and the y-axis diameter d_b is set to 3.5 µm. The length joining the centre of adjacent cladding air holes is denoted as pitch distance p = 4.0816 µm. Furthermore, the ratio between the diameter d_a and pitch distance yields the Air-Filling Fraction (AFF) and specified to 0.98. This high AFF was considered to generate the closest possible distance of cladding air holes to the cladding area to allow total light confinement due to the compactness between the corresponding core and cladding air holes. Furthermore, the total fibre diameter is 32.028 µm, and the PML is configured to be 10% of the cladding diameter, which encloses the cladding and core region.

This proposed sensor for alcohol sensing is an index-guiding PCF sensor that follows the evanescent interaction between light and the sample (Arif and Biddut, 2017). The

https://doi.org/10.6703/IJASE.202306_20(2).001

schematic diagram of the sensing setup is presented in the Fig. 2. Rifat et al. (2017) introduced this experimental procedure that utilizes a light source, the proposed PCF connected between single mode fibres (SMF), optical spectrum analyser (OSA), and a computer. The light source is incident to the PCF core through the aid of the SMF. The OSA is used to monitor the output after proper light-analyte interaction, which is then analysed by a computer.

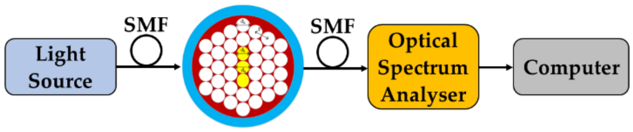

Fig. 2. Schematic diagram for PCF sensing procedure

3. METHODOLOGY

The full vector Finite Element Method (FEM) based simulation process on COMSOL Multiphysics version 5.6 was used to study each variable in determining the performance of the proposed PCF. This simulation method generates a mesh analysis from the derivation of Maxwell's equation whereby numerous elements have been produced: 12081 mesh vertices, 23828 triangular elements, 2204 edge elements and 154 vertex elements. For the objective of the study in evaluating an alcohol detecting PCF sensor, three test analytes were selected: propanol, butanol and pentanol. Also, a range of operating wavelengths has been specified from 0.8 to 2.0 μm. The following table presents the refractive indices of propanol, butanol and pentanol with respect to operating wavelengths.

Table 1. Refractive indices of propanol, butanol and pentanol with respect to operating wavelengths

Wavelength	Material and Analyte Refractive Index			
(μm)	Silica	Propanol	Butanol	Pentanol
0.8	1.4533	1.3786	1.3910	1.4025
0.9	1.4518	1.3776	1.3897	1.4014
1.0	1.4504	1.3768	1.3888	1.4005
1.1	1.4492	1.3761	1.3880	1.3998
1.2	1.4481	1.3756	1.3874	1.3993
1.3	1.4469	1.3750	1.3869	1.3988
1.4	1.4458	1.3745	1.3864	1.3983
1.5	1.4446	1.3741	1.3860	1.3979
1.6	1.4434	1.3730	1.3852	1.3974
1.7	1.4422	1.3724	1.3844	1.3968
1.8	1.4409	1.3716	1.3836	1.3960
1.9	1.4395	1.3707	1.3828	1.3955
2.0	1.4381	1.3698	1.3819	1.3949

To properly establish the sensing potential of the proposed PCF, the following optical properties are evaluated: effective refractive index, birefringence, power fraction, relative sensitivity, confinement loss, effective area and nonlinear coefficient.

The effective refractive index n_{eff} of the silica background material and the supplementary injected core holes can be modelled using Sellmeier's equation (Akowuah et al., 2012):

$$n_{\mathrm{eff}}(\lambda) = \sqrt{1 + \frac{A_1\lambda^2}{\lambda^2 - B_1} + \frac{A_2\lambda^2}{\lambda^2 - B_2} + \frac{A_3\lambda^2}{\lambda^2 - B_3}} \quad (1)$$

where λ is the operating wavelength, $A_{(i=1,2,3)}$ and $B_{(i=1,2,3)}$ are Sellmeier coefficients of that material.

Birefringence Δ occurs in asymmetrical core holes and measures the polarisation of light in the different axes. It can be specified by the difference in effective refractive indices of both x- and y-polarisation of light (Arif et al., 2019; Yakasai et al., 2019a; Agbemabiese and Akowuah, 2020):

$$\Delta = \left|n_{eff}^{x} - n_{eff}^{y}\right| \quad (2)$$

where n_{eff}^{x} is effective refractive index in the x-polarisation of light whereas n_{eff}^{y} is the effective refractive index in the y-polarisation of light.

Power fraction F is determined as the power transmitting in the PCF and can be defined as the ratio of power in a core region to the overall fibre, which can be evaluated as (Maidi et al., 2021b; Yakasai et al., 2019a; Yakasai et al., 2019b):

$$F = \frac{(sample) \int Re(E_x H_y - E_y H_x) dxdy}{(total) \int Re(E_x H_y - E_y H_x) dxdy} \times 100 \quad (3)$$

where E_x and H_x are the electric and magnetic field in the transverse direction, whilst E_y and H_y are the electric and magnetic field in the longitudinal direction. *Re* means the real component of electric field E and magnetic field H.

Relative sensitivity R represents the effectiveness of light interaction in the PCF between the light signal and the test analyte, which is expressed as (Yakasai et al., 2019a; Yakasai et al., 2019b; Maidi et al., 2021b):

$$R = \frac{n_{\mathrm{r}}}{n_{\mathrm{eff}}} \times F \quad (4)$$

where n_{r} is the refractive index of the sensed material.

In a practical sense, light propagating in the core of the fibre may escape to the surrounding cladding region and a portion of a signal is lost. This is confinement loss L and is quantified by (Begum et al., 2009; Begum and Abas, 2019; Yakasai et al., 2020; Maidi et al., 2021a):

$$L = \frac{40\pi}{\ln(10)\lambda} Im[n_{\mathrm{eff}}] \times 10^6 \quad (5)$$

where $Im[n_{\mathrm{eff}}]$ is the imaginary part of the effective mode index.

Effective area A_{eff} represents the intensity distribution of the power propagating in the cross-sectional area of the PCF, and computed by (Begum et al., 2009; Kaijage et al., 2013; Begum and Abas, 2019; Yakasai et al., 2019b):

$$A_{\text{eff}} = \frac{\left(\int_{-\infty}^{\infty}\int_{-\infty}^{\infty}|E|^2\,dx\,dy\right)^2}{\int_{-\infty}^{\infty}\int_{-\infty}^{\infty}|E|^4\,dx\,dy} \tag{6}$$

where E is the transverse electric fields of the guided mode.

Nonlinear coefficient is the quantification of the strength of a nonlinear interaction within the optical fibre and defined as (Hossain et al., 2018; Begum and Abas, 2019; Kumar et al., 2020):

$$\gamma = \left(\frac{2\pi}{\lambda}\right)\left(\frac{n_2}{A_{\text{eff}}}\right) \tag{7}$$

where λ is the operating wavelength and n_2 is the non-linear refractive index

4. RESULTS AND DISCUSSION

The proposed PCF has been analysed to obtain numerical results of optical parameters involving effective refractive index, birefringence, power fraction, relative sensitivity, confinement loss, effective area, and nonlinear coefficient. The COMSOL software was utilised to perform the simulation process to assess the results of the parameters for the wavelength range from 0.8 to 2.0 µm.

Fig. 3 represents the effective refractive index in two polarisations (*x*- and *y*-polarisation) of propanol, butanol and pentanol for the proposed PCF. The graph demonstrates that the effective refractive indices of all three alcohol analytes decrease gradually as wavelength increases. This trend is on the account of lower wavelengths propagating at larger refractive index. Pentanol possesses the highest effective refractive index, followed by butanol and propanol. Additionally, the polarisation in the proposed PCF is minute, where the difference of effective refractive indices between *x*-polarisation and *y*-polarisation are very small. With that, the optical parameters of this study are obtained at the *x*-axis only.

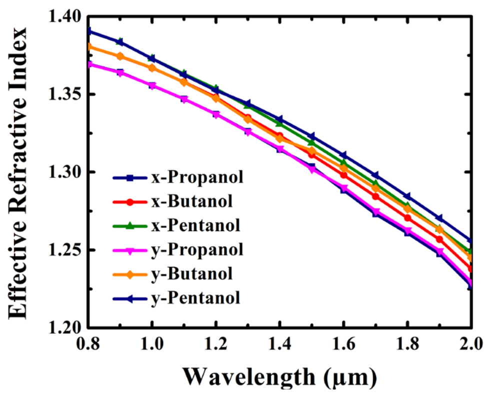

Fig. 3. Effective refractive index in *x*- and *y*-polarisation of the proposed PCF sensor for propanol, butanol and pentanol at operating wavelengths of 0.8 to 2.0 µm

The core structure comprised of elliptical holes that are asymmetrical in both the *x*- and *y*-plane. This design produces birefringence due to the different propagation occurring in its respective direction: *x*-polarisation and y-polarisation. Fig. 4 illustrates the birefringence for all the test analytes: propanol, butanol and pentanol, with respective to operating wavelength. The birefringence of the alcohol analytes are considered linear in the earlier operating wavelengths and gradually increases as the wavelength increases to 2.0 µm. It is noted that minimal birefringence occurs for the proposed PCF design as the values are lower than 0.008. At 0.8 µm optimum wavelength, the birefringence of propanol, butanol and pentanol are recorded to be 0.0001.

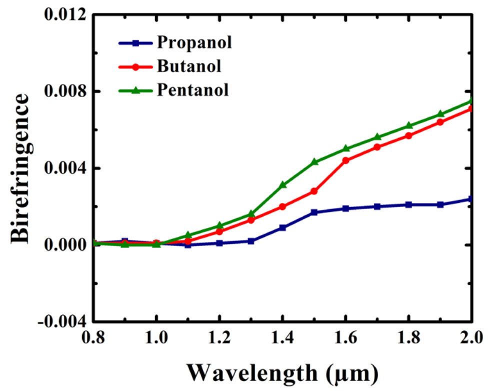

Fig. 4. Birefringence of the proposed PCF sensor for propanol, butanol and pentanol at operating wavelengths of 0.8 to 2.0 µm

Fig. 5 displays the fractional amount of power propagating through the proposed PCF over the core-cladding ratio. It can be observed that the power fraction of the test analytes drastically decrease initially as wavelength increases and slightly decreases further until 2.0 µm. This prevails as optical power flowing in the core diminishes gradually as wavelength increases. At the optimum wavelength of 0.8 µm, the power fraction is recorded to be 92.7%, 88.0% and 81.5% for propanol, butanol and pentanol, respectively.

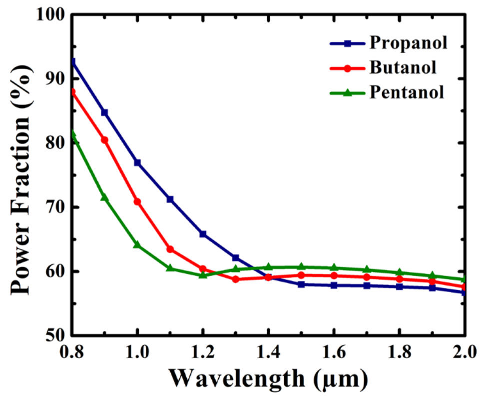

Fig. 5. Power fraction of the proposed PCF sensor for propanol, butanol and pentanol at operating wavelengths of 0.8 to 2.0 µm

In relation to the power fraction obtained, relative sensitivity of the selective alcohol analytes against the operating wavelength is presented in Fig. 6. Since power fraction is a factor of relative sensitivity, it depicts a similar trend to the fractional power results. Propanol, butanol and pentanol obtained relative sensitivities of 93.3%, 88.7% and 82.2%, respectively, at 0.8 μm.

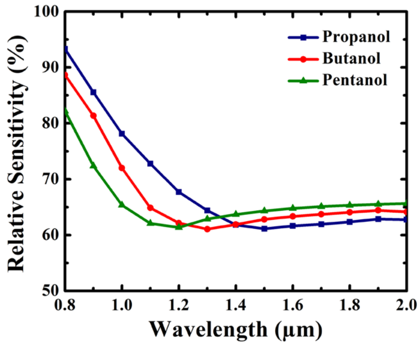

Fig. 6. Relative sensitivity of the proposed PCF sensor for propanol, butanol and pentanol at operating wavelengths of 0.8 to 2.0 μm

Fig. 7 determines the confinement loss of propanol, butanol and pentanol with respect to the operating wavelengths. Generally, the confinement loss increases along with operating wavelength by the reason of electromagnetic waves with high frequency favouring to transmit through high refractive indexed regions (Iqbal et al., 2020). It can be noted that the confinement loss of all three analytes increases gradually as the operating wavelength increases from 0.8 to 2.0 μm. The proposed PCF has assessed confinement losses of $9.80 \times 1/10^{13}$ dB/m for propanol, $4.91 \times 1/10^{13}$ dB/m for butanol and $1.03 \times 1/10^{13}$ dB/m for pentanol at a wavelength of 0.8 μm.

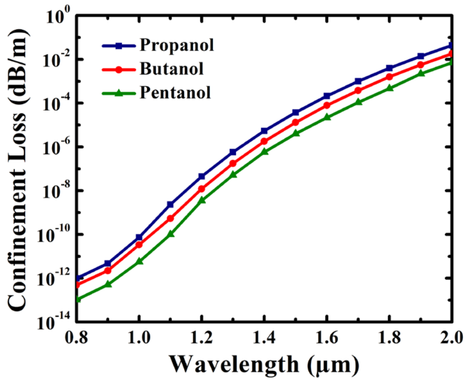

Fig. 7. Confinement loss of the proposed PCF sensor for propanol, butanol and pentanol at operating wavelengths of 0.8 to 2.0 μm

Effective areas of propanol, butanol and pentanol for the proposed PCF with respect to wavelength is illustrated in Fig. 8. Theoretically, effective areas of the fundamental mode profile increase due to less light confined within the core region of the fibre as wavelength increases. Similar trends occur in this fibre sensor design as seen in the figure, where the effective area of propanol, butanol and pentanol increases exponentially as wavelength increases. The effective areas at 0.8 μm wavelength are 0.03839 μm^2, 0.04486 μm^2 and 0.05591 μm^2 for propanol, butanol and pentanol, respectively.

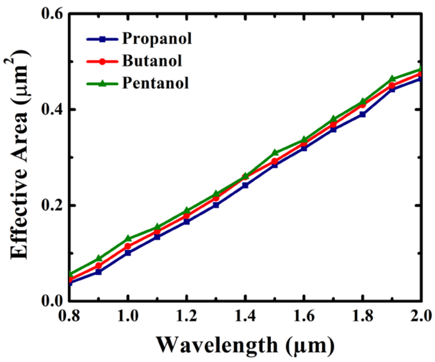

Fig. 8. Effective area of the proposed PCF sensor for propanol, butanol and pentanol at operating wavelengths of 0.8 to 2.0 μm

The graphical representation of the nonlinear coefficient with respect to operating wavelength from 0.8 to 2.0 μm is shown in Fig. 9. It can be observed that the nonlinearity of propanol, butanol and pentanol decreases exponentially as the wavelength increases. Propanol has higher nonlinear coefficients as compared to the other alcohol test analytes. Additionally, nonlinear coefficient is inversely correlated with effective area, where the opposing behaviour is proven in Figs. 8 and 9. At operating wavelength of 0.8 μm, the nonlinear coefficients yield 5939 /Wkm for propanol, 5254 /Wkm for butanol and 4215 /Wkm for pentanol.

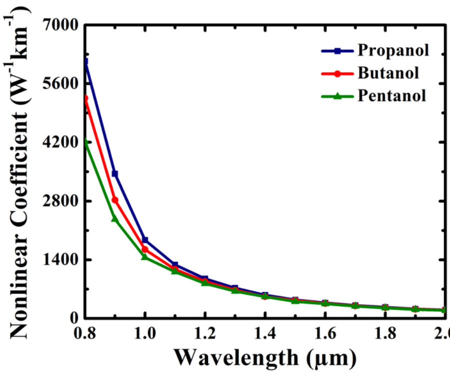

Fig. 9. Nonlinear coefficient of the proposed PCF sensor for propanol, butanol and pentanol at operating wavelengths of 0.8 to 2.0 μm

Furthermore, the results of the proposed alcohol PCF sensor are differentiated to the performance of previous PCFs and presented in Table 2. To contrast, the proposed PCF attained high relative sensitivities and lowest confinement losses for the selected test analytes.

Table 2. Performance evaluation table between previous PCFs and proposed PCF

	Relative Sensitivity (%)			Confinement Loss (dB/m)		
	Propanol	Butanol	Pentanol	Propanol	Butanol	Pentanol
Ref. (Habib et al., 2021)	80.74	84.34	-	$\sim 1/10^{10}$	$\sim 1/10^{11}$	-
Ref. (Ahmed et al., 2017)	65.95	66.35	66.73	$\sim 1/10^{10}$	$\sim 1/10^{10}$	$\sim 1/10^{11}$
Ref. (Ahmed et al., 2017)	58.17	58.74	59.59	$\sim 1/10^{10}$	$\sim 1/10^{11}$	$\sim 1/10^{10}$
Ref. (Ahmed et al., 2019)	41.29	41.30	41.32	-	-	-
Ref. (Paul et al., 2017)	65.44	66.02	66.39	$\sim 1/10^{6}$	$\sim 1/10^{10}$	$\sim 1/10^{9}$
Proposed PCF	93.30	88.70	82.20	$\sim 1/10^{13}$	$\sim 1/10^{13}$	$\sim 1/10^{13}$

5. CONCLUSION

The proposed PCF comprises three oval core holes and three rings circular cladding holes in a hexagon-shaped arrangement to sense alcohols. PML region made up of 10% of the cladding area, whereas the optimum wavelength for each analyte is 0.8 μm. To enumerate, the proposed PCF exhibits high relative sensitivities of 93.3% for propanol, 88.7% for butanol and 82.2% for pentanol, low confinement losses of $9.80 \times 1/10^{13}$ dB/m for propanol, $4.91 \times 1/10^{13}$ dB/m for butanol and $1.03 \times 1/10^{13}$ dB/m for pentanol. The polarisation of light in the x-axis and y-axis is minute, thus, the birefringence obtained is about 0.0001 at the optimum wavelength, for all the alcohol analytes. The simple design coupled with remarkable waveguiding and sensing results determines its practicability in a sensing application, primarily alcohol detection. Moreover, this proposed PCF is applicable in supercontinuum generation because of the high nonlinear coefficient.

ACKNOWLEDGMENT

This research would like to thank the support of Universiti Brunei Darussalam.

REFERENCES

Abdullah-Al-Shafi, M., Sen, S. 2020. Design and analysis of a chemical sensing octagonal photonic crystal fiber (O-PCF) based optical sensor with high relative sensitivity for terahertz (THz) regime. Sensing and Bio-Sensing Research, 29, 100372.

Agbemabiese, P. A., Akowuah, E.K. 2020. Numerical analysis of photonic crystal fiber of ultra-high birefringence and high nonlinearity. Scientific Reports, 10, 21182.

Ahmed, K., Haque, M.J., Jabin, M.A., Paul, B.K., Amiri, I.S., Yupapin, P. 2019. Tetra-core surface plasmon resonance based biosensor for alcohol sensing. Physica B: Condensed Matter, 570, 48–52.

Ahmed, K., Paul, B.K., Chowdhury, S., Islam, M.S., Sen, S., Islam, M.I., Asaduzzaman, S., Bahar, A.N., Miah, M.B.A. 2017. Dataset on photonic crystal fiber based chemical sensor. Data in Brief, 12, 227–233.

Akowuah, E.K., Gorman, T., Ademgil, H., Haxha, S., Robinson, G.K., Oliver, J.V. 2012. Numerical analysis of a photonic crystal fiber for biosensing applications. IEEE Journal of Quantum Electronics, 48, 1403–1410.

Arif, M.F.H., Biddut, M.J.H. 2017. A new structure of photonic crystal fiber with high sensitivity, high nonlinearity, high birefringence and low confinement loss for liquid analyte sensing applications. Sensing and Bio-Sensing Research, 12, 8–14.

Arif, M.F.H., Hossain, M.M., Islam, N., Khaled, S.M. 2019. A nonlinear photonic crystal fiber for liquid sensing application with high birefringence and low confinement loss. Sensing and Bio-Sensing Research, 22, 100252.

Begum, F., Abas, P.E. 2019. Near infrared supercontinuum generation in silica based photonic crystal fiber. Progress In Electromagnetics Research C, 89, 149–159.

Begum, F., Namihira, Y., Razzak, S.M.A., Kaijage, S.F., Hai, N.H., Miyagi, K., Higa, H., Zou, N. 2009. Flattened chromatic dispersion in square photonic crystal fibers with low confinement losses. Optical Review, 16, 54–58.

Habib, M.A., Anower, M.S., AlGhamdi, A., Faragallah, O.S., Eid, M.M.A., Rashed, A.N.Z. 2021. Efficient way for detection of alcohols using hollow core photonic crystal fiber sensor. Optical Review, 28, 383–392.

Habib, M.A., Anower, M.S., Hasan, M.R. 2017. Ultrahigh birefringence and extremely low loss slotted-core microstructure fiber in terahertz regime. Current Optics and Photonics, 1, 567–572.

Hemalatha, R., Revathi, S. 2020. Photonic crystal fiber for sensing application. International Journal of Engineering and Advanced Technology, 9, 481–494.

Hossain, M., Podder, E., Adhikary, A., Al-Mamun, A. 2018. Optimized hexagonal photonic crystal fibre sensor for glucose sensing. Advances in Research, 13, 1–7.

Iqbal, F., Biswas, S., Bulbul, A.A.-M., Rahaman, H., Hossain, M.B., Rahaman, M.E., Awal, M.A. 2020. Alcohol sensing and classification using PCF-based sensor. Sensing and Bio-Sensing Research, 30, 100384.

Islam, S., Kumar, B., Ahmed, K. 2018. Liquid-infiltrated photonic crystal fiber for sensing purpose : Design and analysis. Alexandria Engineering Journal, 57, 1459–1466.

Kaijage, S.F., Ouyang, Z., Jin, X. 2013. Porous-core photonic crystal fiber for low loss terahertz wave guiding. IEEE Photonics Technology Letters, 25, 1454–1457.

Knight, J.C., Birks, T.A., Russell, P.S.J., Atkin, D.M. 1996. All-silica single-mode optical fiber with photonic crystal cladding. Optics Letters, 21, 1547.

Kumar, P., Fiaboe, K.F., Roy, J.S. 2020. Design of nonlinear photonic crystal fibers with ultra-flattened zero dispersion for supercontinuum generation. ETRI Journal, 42, 282–291.

Maidi, A.M., Abas, P.E., Petra, P.I., Kaijage, S., Zou, N., Begum, F. 2021a. Theoretical considerations of photonic crystal fiber with all uniform-sized air holes for liquid sensing. Photonics, 8, 249.

Maidi, A.M., Shamsuddin, N., Wong, W.-R., Kaijage, S., Begum, F. 2022. Characteristics of ultrasensitive hexagonal-cored photonic crystal fiber for hazardous chemical sensing. Photonics, 9, 38.

Maidi, A.M., Yakasai, I., Abas, P.E., Nauman, M.M., Apong, R.A., Kaijage, S., Begum, F. 2021b. Design and simulation of photonic crystal fiber for liquid sensing. Photonics, 8, 16.

Nivedha, S., Senthilnathan, K. 2020. Design of a terahertz alcohol sensor using a steering-wheel microstructured photonic crystal fiber. IETE Journal of Research, 1–9.

Paul, B.K., Islam, M.S., Ahmed, K., Asaduzzaman, S. 2017. Alcohol sensing over O+E+S+C+L+U transmission band based on porous cored octagonal photonic crystal fiber. Photonic Sensors, 7, 123–130.

Podder, E., Hossain, M.B., Al-Mamun Bulbul, A., Shekhar Mondal, H. 2020. Ethanol detection through photonic crystal fiber, 175–182.

Rifat, A.A., Ahmed, R., Mahdiraji, G.A., Adikan, F.R.M. 2017. Highly sensitive D-shaped photonic crystal fiber-based plasmonic biosensor in visible to Near-IR. IEEE Sensors Journal, 17, 2776–2783.

Sen, S., Abdullah-Al-Shafi, M., Sikder, A.S., Hossain, M.S., Azad, M.M. 2021. Zeonex based decagonal photonic crystal fiber (D-PCF) in the terahertz (THz) band for chemical sensing applications. Sensing and Bio-Sensing Research, 31, 100393.

Sultana, J., Islam, M.S., Ahmed, K., Dinovitser, A., Ng, B. W.-H., Abbott, D. 2018. Terahertz detection of alcohol using a photonic crystal fiber sensor. Applied Optics, 57, 2426.

Yakasai, I., Abas, P.E., Kaijage, S.F., Caesarendra, W., Begum, F. 2019a. Proposal for a quad-elliptical photonic crystal fiber for terahertz wave guidance and sensing chemical warfare liquids. Photonics, 6, 78.

Yakasai, I.K., Abas, P.E., Ali, S., Begum, F. 2019b. Modelling and simulation of a porous core photonic crystal fibre for terahertz wave propagation. Optical and Quantum Electronics, 51, 1–16.

Yakasai, I.K., Abas, P.E., Suhaimi, H., Begum, F. 2020. Low loss and highly birefringent photonic crystal fibre for terahertz applications. Optik, 206, 164321.